Competitive partitioning of rotational energy in gas ensemble equilibration

Article (Published Version)

Competitive partitioning of rotational energy in gas ensemble equilibration

Anthony J. McCaffery and Richard J. Marsh

Citation: J. Chem. Phys. **136**, 024307 (2012); doi: 10.1063/1.3675638
View online: http://dx.doi.org/10.1063/1.3675638
View Table of Contents: http://jcp.aip.org/resource/1/JCPSA6/v136/i2
Published by the AIP Publishing LLC.

Competitive partitioning of rotational energy in gas ensemble equilibration

Anthony J. McCaffery[1,a)] and Richard J. Marsh[2]
[1]*Department of Chemistry, University of Sussex, Brighton BN1 9QJ, United Kingdom*
[2]*Department of Physics, University College, London WC1E 6BT, United Kingdom*

(Received 26 August 2011; accepted 16 December 2011; published online 9 January 2012)

A wide-ranging computational study of equilibration in binary mixtures of diatomic gases reveals the existence of competition between the constituent species for the orbital angular momentum and energy available on collision with the bath gas. The ensembles consist of a bath gas AB(v;j), and a highly excited minor component CD(v′;j′), present in the ratio AB:CD = 10:1. Each ensemble contains 8000 molecules. Rotational temperatures (T_r) are found to differ widely at equilibration with T_r^{AB}/T_r^{CD} varying from 2.74 to 0.92, indicating unequal partitioning of rotational energy and angular momentum between the two species. Unusually, low values of T_r are found generally to be associated with diatomics of low reduced mass. To test effects of the equi-partition theorem on low T_r we undertook calculations on HF(6;4) in N_2(0;10) over the range 100–2000 K. No significant change in T_r^{N2}/T_r^{HF} was found. Two potential sources of rotational inequality are examined in detail. The first is possible asymmetry of $-\Delta j$ and $+\Delta j$ probabilities for molecules in mid- to high j states resulting from the quadratic dependence of rotational energy on j. The second is the efficiency of conversion of orbital angular momentum, generated on collision with bath gas molecules, into molecular rotation. Comparison of these two possible effects with computed T_r^{AB}/T_r^{CD} shows the efficiency factor to be an excellent predictor of partitioning between the two species. Our finding that T_r values for molecules such as HF and OH are considerably lower than other modal temperatures suggests that the determination of gas ensemble temperatures from Boltzmann fits to rotational distributions of diatomics of low reduced mass may require a degree of caution. © *2012 American Institute of Physics*. [doi:10.1063/1.3675638]

I. INTRODUCTION

Recent state-to-state computational studies[1–4] of equilibration in gas ensembles have shown the thermalisation process to be far from straightforward. This view is the result of a series of investigations in which ensembles containing a subset of highly excited diatomic molecules are deactivated by various diatomic bath gases in their ground states. Equilibration is generally multi-staged and often the component species modal temperatures (T_m) have not become equal after more than 1000 collision cycles despite the ensemble apparently being at equilibrium. This latter effect can be particularly striking for the rotational temperature (T_r) since the equilibrated T_r value for some species is often found to be much the lower than all other T_m present. This is very marked for molecules such as OH.[3,4] When OH in $v_{OH} = 8$; $n_{OH} = 6$ (abbreviated to OH(8;6) or to OH*) equilibrates in a mixture of N_2(0;10) and O_2(0;12), T_r for OH eventually falls below all other T_m and from around 300 collision cycles becomes the lowest of all nine possible modal temperatures by at least 500 K.

This phenomenon may be of wide significance. OH is an important component in combustion[5] and in the industrial plasmas of welding[6] and vapour deposition and numerous laser-based techniques have been devised to determine the concentration and spatial distribution of OH.[5] Measured OH rotational state distributions are often used as a remote indicator of the kinetic temperature (T_t) of a gas ensemble, with the implicit assumption that thermodynamic equilibrium has been reached between rotation and translation modes. This method is widely used in atmospheric science[7] using spectrally resolved OH emission, known since the 1950s to be[8] a component of Earth's airglow. A wide variety of air-borne and ground-based monitoring methods have been developed to measure OH rotational temperatures as described in a recent definitive survey by Cosby and Slanger.[9] Our finding[3,4] that T_r of OH at equilibrium is considerably lower than that for N_2 and O_2, and generally much lower than the vibrational (T_v) and translational (T_t) temperatures of each species present, suggests that the use of Boltzmann fits to rotational distributions to determine kinetic temperature may require a degree of caution.

In this article we address a number of questions raised by the unexpectedly low value of T_r predicted for OH by our ensemble relaxation model. These fall into distinct categories which are, in brief, (i) is the effect real, (ii) what is its relevance to real-life situations (iii) if real, how widespread is the phenomenon, and (iv) what might be its cause? Before beginning discussion, question (iii) is partially answered by demonstrating that unexpectedly low T_r values are also found in ensembles consisting of HF* in a bath of N_2. This is seen from Fig. 1 in which the relaxation of HF(6;4), the minor constituent in a bath of N_2(0;10), T_m is plotted as a function of

a)Author to whom correspondence should be addressed. Electronic mail: A.J.McCaffery@sussex.ac.uk.

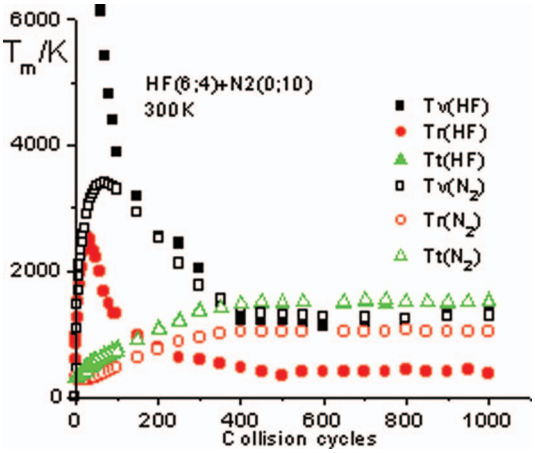

FIG. 1. Modal temperature (T_m) plotted against number of collision cycles for HF (6;4), present as an approximately 10% component in N_2 (0;10) at an initial temperature of 300 K. Ensemble size is (nominally) 8000 molecules. Vibrations are represented by squares, rotations by circles, and translations by triangles. HF modal symbols are filled and those for N_2 are open.

number of collision cycles. Note that here the term collision cycle refers to a process in which all molecules in the ensemble undergo a single collision on average. It is clear therefore that well before the point of apparent equilibration of the ensemble is reached, T_r for HF becomes the mode of lowest temperature. Thus, the phenomenon of exceptionally low T_r for one species in an ensemble is not limited to the case of OH.

The distinctive features found in ensembles containing OH* are also present in those consisting of HF* in N_2 as Fig. 1 clearly displays. The most striking similarities include the relatively rapid fall of T_v for HF* as it exchanges vibrational quanta with the bath gas. Pathways of low *total* energy change exist such as the coupled transitions $\{v_{HF} = 6 \rightarrow 1$ or 2; $v_{N2} = 0 \rightarrow 9$ or 7$\}$ to rapidly deactivate HF*. More significant, however, is the behaviour of T_r for HF. As in the case of OH (Refs. 3 and 4) there is an initial sharp rise in rotational temperature, primarily due to population redistribution via the mechanism of quasi-resonant vibration-rotation transfer (QVRT).[3] This process has been described in detail in the context of OH and involves simultaneous vibrational relaxation with rotational excitation or vice-versa, the latter only after population has begun to spread across the v_{HF} levels. The high j_{HF} states populated during this phase are slowly relaxed over many collisions and eventually T_r for HF becomes the lowest of the six energy modes available in this ensemble. The value of T_r for HF averaged over the final 500 collision cycles is 380 K, while the next lowest T_m is T_r for N_2 at 1030 K.

The above example demonstrates that once the major energy redistribution processes have occurred, the drop of T_r to well below the T_m of other species present is not limited to ensembles containing OH. Here we present a wider, more systematic, study of this finding to address the questions raised above. The computational model used here and in earlier article[1–4,10] represents the first attempt to predict state-to-state energy flow in gas mixtures as a function of number of collision cycles. Relatively little experimental data exist against which to calibrate our predictions and our discovery of what appear to be collisionally super-cooled OH and HF rotational distributions in certain bath molecules raises a number of questions.

This article is structured as follows. First, we describe a critical analysis of methods employed to obtain the data contained in plots such as Fig. 1. This includes a brief review of previous findings and experimental evidence that supports our calculated results. Second, we discuss the relevance of our data, obtained using a thermodynamically closed system, to real-life environments such as planetary atmospheres or combustion processes. Third, possible mechanisms that might lead to competition for rotational energy, and hence excess rotational cooling of molecules such as OH or HF, are considered as part of a wider survey of the phenomenon of apparent rotational competition.

II. DESCRIPTION AND CRITICAL ANALYSIS OF METHODOLOGY

A. Theoretical basis

The basis of the computational routine is the angular momentum (AM) model of state-to-state inelastic collisions. Two recent reviews[11] describe the formulation and development of this model and its application to a wide range of state-to-state collision-induced processes in molecules. More relevant to this work is the derivation of equations of collision-induced energy and AM transfer for the general atom–diatom[12] case and those that govern the more complex diatom–diatom collision.[13] These articles[12,13] describe a computational method based on a 3D ellipsoidal shape or *Newton surface*, the purpose of which is to mimic a diatomic molecule in converting linear momentum of relative motion to orbital and rotational angular momentum. The dimensions of the Newton surface are determined by the bond length of the diatomic[12] so that a-b = half bond length, 2a = bond length, where a and b are ellipsoid semi-major and semi-minor axes, respectively. A large number of random trajectories are run for each application, an approach that was first introduced by Kreutz and Flynn.[14]

In the simplest form, two equations form the basis of the theoretical method, the first expressing conversion of linear-to-orbital angular momentum on impact at the Newton surface. This initial orbital AM is partitioned between molecular rotation and recoil orbital AM. The generation of angular momentum is via a lever-arm, or effective impact parameter (b_n), whose maximum length (b_n^{max}) in atom–diatom collisions is half bond length, or the equivalent distance(s) from the centre-of-mass in heteronuclear species. This changes for diatom–diatom collisions where now the maximum lever arm may take all values up to the sum of the b_n^{max} values of the two species involved.[13] The second equation expresses state-to-state energy conservation for the conversion of kinetic energy of relative motion into internal (v;j) energy for each initial-to-final quantum state transition. These two equations contain the principal expressions of conservation of energy and angular momentum for each state-to-state transition. The diatom–diatom formulation[13] is the basis of much of the work

described here with expressions for angular momentum change, Δj_a and Δj_b in diatomics a and b, under conditions set by state-to-state energy conservation,[13]

$$\Delta j_a = \frac{2\mu_{ab} b_{na}(I_a I_b v_n - I_a b_{nb}|j_b|\cos\beta - I_b b_{na}|j_a|\cos\alpha)}{I_a I_b + I_b \mu b_{na}^2 + I_a \mu b_{nb}^2}, \quad (1)$$

$$\Delta j_b = \frac{2\mu_{ab} b_{nb}(I_a I_b v_n - I_a b_{nb}|j_b|\cos\beta - I_b b_{na}|j_a|\cos\alpha)}{I_a I_b + I_b \mu b_{na}^2 + I_a \mu b_{nb}^2}. \quad (2)$$

Here μ_{ab} is the reduced mass of the (a,b) pair of diatomics, b_{na},b_{nb} are the effective impact parameters of the two molecules, I_a, I_b are their moments of inertia, v_n is the normal component of relative velocity, j_a, j_b are the rotational AM vectors, and α or β represent the angle between initial rotational AM vectors of a or b, respectively, with the collision plane defined by v_n and b_n for each ellipsoid. The full derivation of these equations is given in Ref. 13.

The theoretical method focuses on accurate calculation of rotational transition probabilities. Vibrational state populations are considered to be the sum of that state's rotational populations and hence vibrational state change represents a (momentum and energy) barrier that must be overcome before rotational levels within that state may be populated. Thus, the building blocks of this collision theory are the *rotational* transition probabilities. These are summed to obtain a particular vibrational state population and the vibrational states summed to obtain the full electronic state contribution if required. The computational method based on the AM theory has been tested extensively and found to reproduce quantitatively experimental data and that from quantum close-coupled calculations.[12,13] This agreement implies that an ellipsoidal Newton surface of molecular dimensions yields a $P(b_n)$, the probability density function for b_n, closely resembling that of a real diatomic molecule. The $P(b_n)$ function plays a central role in the expression for transition probability, unlike other theoretical methods, computing the state-to-state outcome of single collisions using the AM method is very fast and requires only readily available data such as bond length, atomic mass, spectroscopic constants, and temperature.

B. The computational model

The multi-collision program works in the following manner. Each ensemble consists of up to 10 000 molecules and may contain up to three different diatomic species in any chosen proportion. The different species are set initially in specific (v;j) states, one generally in an excited rovibrational state. Current computations are limited to $v < 10$ and $j < 100$. Input data are atomic mass, spectroscopic constants, and temperature or collision energy. In the computation, a pair of molecules is chosen at random from the initial array and collided at random angle with probability weighted by velocity. The post collision quantum states and velocities are recorded. A second pair is then chosen for this same procedure, then a third and so on until N (the number of molecules present) binary encounters have occurred. This constitutes a complete collision cycle. After each collision cycle the primary data available are vibrational state populations and, separately, the rotational state populations for each of the three species. In addition, the program computes modal temperatures (T_v, T_r, T_t) for each of the three species, with all of the above data available after each collision cycle. Note that the primary data are the quantum state populations. Modal temperatures are not meaningful in the early stages of ensemble evolution when all molecules are in single or a limited range of quantum states. The T_m values become more reliable as the equilibration proceeds. Despite this imprecision, the modal temperatures plotted against number of collision cycles, as, e.g., in Fig. 1, are found to be valuable for categorising different modes and stages of overall equilibration. Note that for a given number of cycles, the number of collisions undergone by the species present is a distribution function centred on the number of collision cycles undergone. This distribution becomes broader as the evolution continues and hence the term "number of collision cycles" refers to the peak of the distribution function representing actual number of collisions undergone.

Although the modal temperatures are not the primary data from our computation, the value of T_r has a particular significance in numerous practical applications because it can often be determined from spectral intensities using remote methods. In such determinations there generally is implicit assumption of local thermodynamic equilibrium, i.e., modal temperatures are taken to have equalised and hence T_r is an accurate estimate of the kinetic temperature of the gaseous environment being probed. Fig. 1 makes clear that the results from our computational model would not seem to support this conclusion since T_r for HF is considerably lower than all other T_m values. A similar result was found in the case of OH in N_2, O_2 or a mixture of these two gases.[3,4] It is of interest to note that T_r for N_2 in Fig. 1 is much closer to the translational temperature at equilibrium and this is found to be the case in other gas ensembles.[1,2] In the computation, T_r values are calculated from the average rotational energy of the relevant species divided by Boltzmann's constant (k). This value of T_r is used in the program to generate a rotational Boltzmann distribution, which is displayed along with the calculated rotational intensities. An example of this output is given in Fig. 2 and is seen to be a quite reasonable, though not exact, representation of the computed data. Figure 2 was obtained while performing calculations[3] on OH* in N_2 and represents the OH rotational distribution after 300 collision cycles, i.e., just as T_r has begun to level out and is close to its final value. The Boltzmann fit is somewhat skewed by the relatively small populations in $n_{OH} = 6$, 7, and 8. If the lower n_{OH} populations alone were to be considered, a misleadingly reduced value of T_r would result. The calculated populations of $n_{OH} = 5$, 6 are small, but they make a substantial contribution to the total rotational energy. A more accurate description of the OH rotational distribution after 300 collision cycles would be Boltzmann-like.

Unreliable computed T_r values from our model might result from failure of the equipartition principle for molecules such as OH and HF, both of which have large rotational constants. This is much less likely to be a problem in computing T_r for N_2 and similar species. The condition under which the equipartition theorem is valid[15] can be expressed in terms of the parameter θ, defined by the relation $k\theta = hcB$, where B

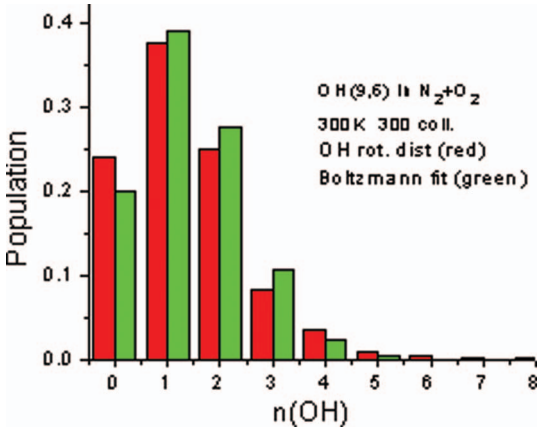

FIG. 2. Rotational distribution among OH molecules (red columns) after 300 collision cycles in a bath of N_2. Initial conditions: OH(8;6) in a bath of $N_2(0;10) + O_2(0;12)$ at 300 K. Ratio of OH* to bath molecules = 1:10. Ensemble size (nominally) 8000 molecules. Boltzmann distribution (green columns) is also shown at the T_r value calculated by the program in the manner described in the text.

is the rotational constant of the molecule concerned. In statistical terms, high temperature is defined to be when $T_t \gg \theta$. Values of θ for OH and HF are 27.2 K and 30.1 K, respectively. The *initial* value of T_t at 300 K is an order of magnitude greater than θ for OH and HF and therefore these molecules might be considered marginal. However, after 300 collision cycles, T_t has risen to near 1500 K for each of these species in the ensembles examined so that the equipartition criterion can be assumed to be met in the mid- to late stages of ensemble equilibration when T_r is found to drop dramatically below other modal temperatures. To verify the assertion that the equipartition criterion, or other factors such as rounding or computational errors influence the computer T_r values, we have carried out a series of computations on HF (6;3) in a bath of N_2 (0,10) over a wide range of initial temperatures from 100 K to 2000 K. The data from these calculations are shown below in Table I.

Several points emerge from this temperature dependent study of HF* in N_2 and in HF.

(1) T_r for HF increases as the amount of energy within the system increases but remains a near constant proportion of translational temperature over the range 100–2000 K. This indicates that concerns regarding the validity of the equipartition principle in the calculation of T_r for molecules such as HF and OH are likely to be groundless.
(2) The data indicate that storage of rotational energy and AM occurs preferentially in N_2 rather than in HF. Within the ensemble, disposal of angular momentum and energy generated on collision with the predominant bath species appears to be competitive, with N_2 much more successful than HF.
(3) Conversion of translational energy and linear momentum to rotational energy and rotational AM in HF is ineffective in HF(0;0) + HF(0;0) collisions even at T_t = 2000 K. By contrast, conversion occurs readily in $N_2(0;0) + N_2(0;0)$ collisions.
(4) The partitioning of rotational AM and energy between HF(0;0) and N_2(0;0) at 2000 K is in the same proportion to that found when the initial excess energy is largely contained within a single HF(v;j) quantum state.

C. Comparison with experiment

Quantum state-resolved experiments designed explicitly to determine the evolution of state populations or modal temperatures in gas mixtures as a precise function of number of collisions have yet to be performed. As a result, direct comparison of our predicted T_m evolution with experiment is not possible except in a limited and indirect manner. For example, both HF and OH have been used as the gain media in chemical lasers,[16,17] devices that operate under multi-collision conditions – generally in a buffer of rare gas atoms. These species are formed rovibrationally hot from highly exothermic

TABLE I. Temperature dependence of equilibrated T_m values (averaged over final 500 collision cycles) for HF (6;3) present in the ratio 1:10 in a bath of N_2(0;10). Total number of molecules is (nominally) 8000. Also tabulated for comparison are results from HF(6;3) + HF(0;3) at 300 K, HF(0;0) + N_2(0;0) at 2000 K, $N_2(0;0) + N_2(0;0)$ at 2000 K, and HF(0;0) + HF(0;0) at 2000 K. The final three columns show ratios T_r^{HF}/T_t^{N2}; T_r^{N2}/T_t^{N2}; and T_r^{N2}/T_r^{HF}.

Collision Temp. (K)	HF T_v	HF T_r	HF T_t	N_2 T_v	N_2 T_r	N_2 T_t	T_r^{HF}/T_t^{N2} (%)	T_r^{N2}/T_t^{N2} (%)	T_r^{N2}/T_r^{HF}
100	1171	370	1414	1170	954	1397	26.5	68.6	2.57
300	1207	397	1520	1280	1042	1521	26.1	68.5	2.62
500	1230	424	1611	1348	1130	1611	26.3	70	2.66
800	1408	529	1796	1464	1260	1778	29.7	71	2.4
1200	1523	610	2008	1593	1416	2008	30	71	2.33
2000	2032	770	2393	1863	1751	2383	32	73.5	2.14
$HF^*(6;3)^+$	HF*	HF*	HF*	HF	HF	HF			
HF(0;3) 300 K	1125	303	2100	1126	300	2093			
$HF(0;0)^+$	HF	HF	HF	N_2	N_2	N_2			
N_2(0;0) 2000 K	1045	316	1506	1110	976	1498	21	65	3.1
$N_2(0;0)^+$	N_2	N_2	N_2	N_2	N_2	N_2			
N_2(0;0) 2000 K	1143	876	1288	1158	866	1293			
HF(0;0)+HF(0;0)	HF	HF	HF	HF	HF	HF			
2000 K	841	250	1801	852	249	1818			

chemical reactions and laser action is observed from a range of states depending on the extent of exothermicity of the initiating reaction. That population inversion has been observed in these two species is not surprising, given the sharp initial rise of T_r for HF* shown in Fig. 1, with similar behaviour highlighted recently for OH*.[3,4] The highly inverted rovibrational populations obtained by Pimentel *et al.*[16] for HF and by Robinson and co-workers[17] in the case of OH are readily reproduced by our model and shown to be the result of QVRT.[3] In addition, our model of OH* in N_2/O_2 was able to reproduce the exceptionally high rotational excitation, $n_{OH} > 30$, previously identified in Earth's airglow[18] as originating from OH molecules in the mesosphere. Once again, the critical mechanism is that of QVRT.[3]

Computer modelling of CO* equilibration in CO (Ref. 19) reproduced several of the key features seen experimentally[20] in laser-induced CO plasmas. However, the limit on our model to $v \leq 10$ means it is not feasible to simulate the conditions found in the experiment, in which population of states having $v_{CO} > 40$ are reached. The computational model was, however, able to confirm the validity of the collisional up-pumping mechanism proposed by Flament *et al.*[20] Hancock and co-workers[21] measured T_m values for $N_2(A^3\Sigma_u^+)$ in a rf plasma and found a T_v values some 3000 K higher than T_r and T_t. Our model of this system[2] gives modal temperatures that agree closely with the measurements of Hancock *et al.* The conditions of this latter experiment,[21] namely, 25 mTorr pressure in a cavity enhanced spectroscopic cell, indicate a regime well beyond the $\sim 10^3$ collisions of our computations, suggesting that the quasi-equilibrium we predicted[2] for N_2* in N_2 may persist through many collisions.

In contrast, the agreement with experimental data obtained by Seeger and Leipertz[22] is less good. These authors measured the rotational temperature of N_2 in air over a wide temperature range using Coherent anti-Stokes Raman spectroscopy techniques and found good agreement between T_r and the temperature recorded by a thermocouple mounted inside the heated chamber. The latter device is insensitive to mode and therefore the discrepancy at 2000 K of ~45 K (Ref. 22) between the two measurements is to be compared to that between T_r of N_2 and the average of the three N_2 modes, which for the 2000 K N_2 data of Table I is ~240 K.

The experiments of Seeger and Leipertz were performed at ambient pressure and represent a collision cycle regime well outside the capabilities of our current model. Graphs such as that shown in Fig. 1 reveal an apparent equilibration in that T_m changes are small in comparison to the values attained – behaviour that continues at least to 2500 collision cycles in N_2 – containing ensembles. The term quasi-equilibrium may be more appropriate form of description for these apparently stable regions of large T_m difference found in our computations and in the experiments of Hancock *et al.*[21] The collision cycle region that would extend to atmospheric pressure and beyond remains to be fully investigated. Further support for the accuracy of our computational model comes from the cross-sections measured by Ottinger *et al.*[23] for state-resolved V-V population exchanges in a nitrogen plasma which are in good agreement with the single (first) collision cross sections we compute for N_2*–N_2 multi-quantum V–V transfer.

Our computational model reproduces a significant number of the principal early features of equilibration in the gas ensembles we have examined. Thus, our prediction of an initial sharp rise in T_r for HF here, and for OH in previous work,[3,4] is likely to be reliable at least for ensemble conditions similar to those we define. This latter caveat concerning conditions of the computational model addresses the second question raised early in Sec. I, i.e., the *relevance* of our predictions to the range of environments in which many collisions occur. Each ensemble in our computational model represents a thermodynamically closed system in which neither energy nor matter may escape. This may be representative of certain experiments in, e.g., some forms of combustion or the confined plasmas of gas lasers. In others, planetary atmospheres, for example, events such as transport of species into and out of the region under consideration, and radiative loss, will influence ensemble evolution. In such circumstances our computed T_m values are unlikely to match exactly those obtained, for example, from measurements of OH spectra in Earth's atmosphere. The model represents an idealised situation with none of the variability in, e.g., temperature, number density, sample size etc. that characterise the difficult experiments carried out by atmospheric scientists.

This absence of environmental variation has the advantage that many key characteristics of the equilibration process may be interpreted in terms of the well-established concepts of collision dynamics Thus, we believe that at least the principal features found in the simulations carry a strong element of reliability despite the relative paucity of confirmatory experimental data. Thus, the predicted rapid rise in T_r for HF and OH is indirectly confirmed as a real phenomenon by the observation of laser action from rovibrational levels in these two species, by the high n_{OH} features seen in Earth's airglow and by the identification of verified mechanisms by which these processes could occur. The unusually low T_r values predicted for HF and OH late in the equilibration process are also very marked features of the simulations but as yet have no equivalent supportive empirical evidence. However, for reasons described in more detail below, we believe it to be a real phenomenon. Furthermore, our findings suggest that T_r values for species such as HF* and OH* evolve in a complex fashion as equilibration proceeds. This potentially has significance in the context of experiments that determine environmental temperatures from OH spectral intensities since, as earlier article[3,4] has demonstrated, T_r and T_t follow very different patterns as OH* equilibrates in the principal atmospheric gases and typically are similar in magnitude only over a very short range of the collision cycle dependence. The stable region from 300–1000 collision cycles is one in which T_r is several hundred degrees Kelvin lower than T_t for this species.

III. ORIGINS OF ROTATIONAL COMPETITION

Unexpectedly low values of T_r for HF and OH in baths of N_2 are not confined to these species and we have found this behaviour to be a general characteristic of molecules having very low reduced mass. The diatomic hydrides are

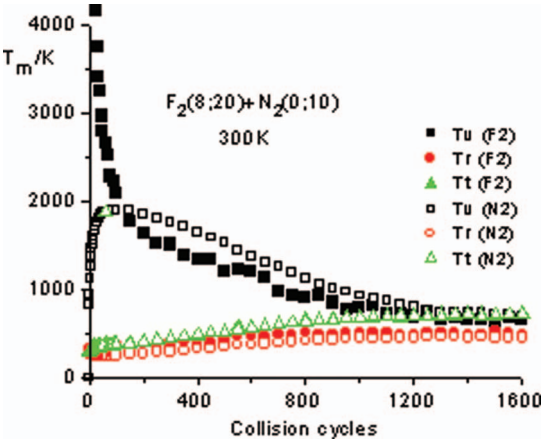

FIG. 3. Modal temperature (T_m) plotted against number of collision cycles for F_2 (8;20), present as an approximately 10% component in N_2 (0;10) at an initial temperature of 300 K. Ensemble size is (nominally) 8000 molecules. Vibrations are represented by squares, rotations by circles, and translations by triangles. F_2 modal symbols are filled and those for N_2 are open.

particular examples of molecules that follow similar patterns of ensemble relaxation to that shown by HF(6;4) in N_2(0;10), illustrated in Fig. 1. In each instance, there is a sharp rise in T_r early in ensemble evolution followed by a fall of this modal temperature to below all others after some 200–300 collision cycles. Other diatomics however follow a very different pattern of equilibration, typified by F_2(8;20) in N_2(0;10) as Fig. 3 illustrates. Here T_r for the initially excited species no longer peaks in the first 50–100 collision cycles but rises very slowly as energy is redistributed. For most of the ensemble's evolution, T_r for F_2 exceeds that for N_2 and both are quite close to other modal temperatures of each species present once the system has equilibrated.

Computations have been carried out on a representative sample of each of the two distinct types of ensemble mentioned above with relevant data shown in Table II. In most examples, N_2 formed the bath gas and in all cases the ratio of excited-to-bath molecules was 1:10 with initial collision energy set as a 300 K Maxwell–Boltzmann distribution. Table II lists the ensembles examined and they are broadly grouped according to the two categories of behaviour represented by Figs. 1 and 3. The table lists rotational temperatures for bath (AB) and excited (CD) molecules and the ratio T_r^{AB}/T_r^{CD}. These represent the mean of readings from the final 500 collisions of the evolution of each ensemble, a region in which little significant T_m change appears to take place in either species. Table II also gives reduced mass values for the AB species. In addition, predictions are listed from calculations of molecular factors that might determine outcomes in the competition for rotational energy and AM. These factors are discussed below in more detail.

Before the discussion, however, we note some key features of Table II. First, the group of six CD molecules at the top of Table II, having reduced mass in the range 0.85–2, are all characterised by a T_r^{AB}/T_r^{CD} ratio lying between 1.8 and 3. This group of molecules all undergo rapid rotational excitation in the early part of ensemble evolution in a manner similar to HF(6;4) in N_2(0;10) in Fig. 1.

A second feature is that when NO, O_2, or F_2 are the excited species in a N_2 bath, T_r for the initially excited molecule is higher than that of the N_2 bath species. Third, the T_r^{AB}/T_r^{CD} ratio is generally close to unity when excited species and bath gas have similar values of reduced mass. Finally, we note that when HF(0;4) is the bath gas and N_2(8;10) the initially excited species, rotational energy, and AM preferentially flow to N_2 so that T_r at equilibrium for this minor component is very high, while HF is again rotationally very cold.

TABLE II. Data obtained from calculations on excited molecules (CD) in bath molecule (AB) for a range of different species. In most cases $^{14}N_2$ is the bath gas. Each ensemble consists of (nominally) 8000 molecules with excited:bath molecule ratio 1:10. The table lists molecular reduced mass as well as mean final rotational temperatures for both excited and bath molecules and their ratio. The final two columns show calculated efficiency factor and energy factor ratios. *See text for definition of these two factors.

Bath mol. (AB)	Excitedmol. (CD)	μ_{CD} (amu)	T_r^{AB} (K)	T_r^{CD} (K)	T_r^{AB}/T_r^{CD}	Efficiency factor* AB/CD	Energy factor* B_{CD}/B_{AB}
N_2(0;10)	LiH(8;6)	0.875	589	320	1.84	1.9	3.8
N_2(0;10)	DCl(8;6)	1.89	882	380	2.32	2.0	2.7
N_2(0;10)	OH(8;6)	0.941	1162	478	2.43	2.4	9.5
N_2(0;10)	HF(6;3)	0.95	1042	397	2.62	2.5	10.5
N_2(0;10)	HCl(8;6)	0.98	1006	381	2.64	2.8	5.3
N_2(0;10)	HI(8;6)	0.99	815	297	2.74	3.3	3.3
N_2(0;10)	LiCl(8;16)	5.83	403	286	1.41	1.2	0.35
N_2(0;10)	CCl(8;16)	8.91	451	419	1.08	0.99	0.35
N_2(0;10)	MgCl(8;20)	14.24	437	440	0.99	0.87	0.12
N_2(0;10)	FCl(8;20)	12.31	294	284	1.03	0.82	0.26
N_2(0;10)	N_2(8;10)	7.0	257	259	1.0	1.0	1.0
N_2(0;10)	NO(8;10)	7.47	737	779	0.95	0.97	0.85
N_2(0;10)	O_2(8;12)	8.0	636	678	0.94	0.93	0.72
N_2(0;10)	F_2(8;20)	9.5	459	499	0.92	0.85	0.45
$^{15}N_2$(0;10)	$^{14}N_2$(0;10)	7.0	320	327	0.98	0.97	1.07
O_2(0;12)	NO(8;10)	7.47	765	742	1.03	1.03	1.1
HF(0;4)	N_2(8;10)	7.0	364	1278	0.28	0.15	0.095

Table II also lists indicators representing attempts to understand the physical causes of what, for certain ensemble combinations, appears to be strong competition for rotational energy and AM between species in binary ensembles. The columns list data that relate to two potential mechanisms, or factors, that might affect rotational state populations and hence, over many collisions, show a bias in the computed T_r^{AB}/T_r^{CD} ratios. These influences are referred to in what follows as (i) the energy factor and (ii) the efficiency factor and definitions of these and justification for their choice are given below.

A. Energy factor

There is an inherent asymmetry in the rotational energy levels of diatomic molecules that, in certain circumstances, could favour relaxation over excitation in collision-induced Δj change. The origin of this effect is the quadratic dependence of rotational energy on quantum number. When $j = 0$, or is small, the momentum of impact will be converted solely, or predominantly, into rotational excitation plus recoil AM. However, when the initial j-state is reasonably high, rotationally inelastic transitions to lower j are likely to dominate as we show below. This selectivity becomes greater as rotational separations increases, i.e., as initial j, or the magnitude of the molecule's rotational constant (B), increase. The effect may be quantified and displayed via velocity–angular momentum diagrams[24] in which the principal equations of energy and of AM conservation are plotted for each $j_i \rightarrow j_f$ transition. The v_r–Δj diagrams represent the threshold state-to-state condition for energy (the E-equation), via the relation

$$|E_f - E_i| = \Delta E = \frac{1}{2}\mu v_r^2, \tag{3}$$

and for AM (the A-equation) through

$$\Delta j = \mu v_r b_n^{max}. \tag{4}$$

These separate expressions for state-to-state energy and AM change assume all collision energy is converted to rotational energy, (Eq. (3)) and all relative linear momentum to rotational AM (Eq. (4)) and thus represent the channel-opening conditions. Note that in all computations, the equations for energy and AM for each state-to-state transition are solved simultaneously.

Figure 4 makes clear that up/down RT asymmetry is predicted on energy grounds since the number of both energy – and AM – permitted velocities, and hence trajectories, is greater for each −ve Δj compared to +ve Δj of the same magnitude. This effect increases as the rotational constant increases so that for HF, all −ve Δj transitions down to −4 are accessible at or near the mean v_r (shown by an up-pointing arrow on the velocity axis), whereas transitions of $+\Delta j > 2$ will be accessed only by velocities well into the high velocity tail of the v_r distribution. The effect of this preference, and/or that of other factors discussed below, is apparent in single collision rotational distributions as Fig. 5 illustrates. This figure shows calculated rotationally inelastic transfer cross sections for gas ensembles comprising (minor component

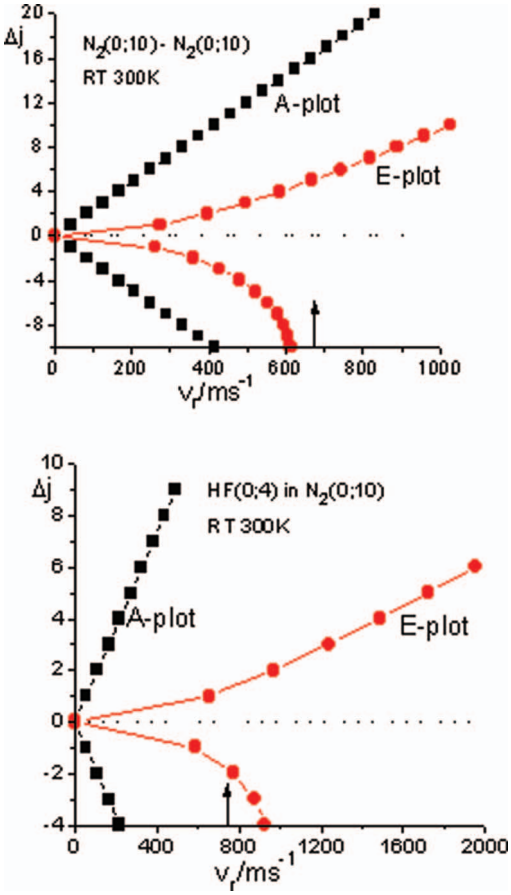

FIG. 4. Velocity–angular momentum diagrams for rotationally inelastic transitions collisions of $N_2(0;10)$–$N_2(0;10)$ (upper graph) and HF (0;4)–$N_2(0;10)$ (lower graph). In each case the energy constraint is dominant so that only velocities greater than those of the E-plots may access individual channels. The up-pointing arrow on each v_r axis marks the mean relative velocity of the collision pair.

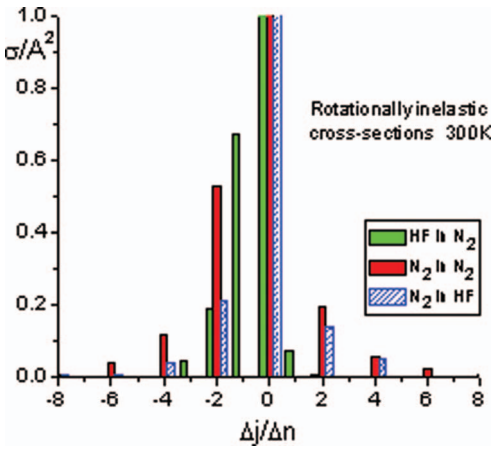

FIG. 5. Rotational transfer cross sections illustrating the $\pm\Delta j$ asymmetry in HF(0;4)–$N_2(0;10)$ and $N_2(0;10)$–$N_2(0;10)$ single collisions and $N_2(0;10)$ in HF(0;4). Elastic $\Delta j = 0$ cross sections are off scale in all three cases illustrated. The probabilities were computed for single collision cycles of gas ensembles with HF(0;4) as minor constituent in $N_2(0;10)$ (green columns), $N_2(0;10)$ as minor constituent in $N_2(0;10)$ (red columns), and $N_2(0;10)$ as minor constituent in HF(0;4) (blue columns).

first) HF(0;4) in N_2(0;10), N_2(0;10) in N_2(0;10) and N_2(0;10) in HF(0;4).

The significant comparisons are between the first two of these pairs of molecules since the majority of collisions undergone by each bath gas molecule will be with another bath gas molecule rather than with one of the minor component. A smaller number of bath gas – minor component collisions will take place and the cross sections for inelastic transfer in these was determined from an ensemble in which N_2(0;10) was the minor component in a bath of HF(0;4). It is evident from Fig. 5 that the $-\Delta j/+\Delta j$ inelastic cross section ratio is very different for these two molecules. Their rotational constants differ markedly with $B_e = 1.998\ cm^{-1}$ for N_2 and $20.956\ cm^{-1}$ for HF.[25] The ratio of the sums of $-\Delta j$ and $+\Delta j$ inelastic cross sections from these calculations was found to be 11.91 for HF in N_2, 2.52 for N_2 in N_2 and 1.83 for N_2 as minor constituent in HF. All calculations were carried out at 300 K.

Thus, the quadratic dependence of rotational state energy on j provides a naturally occurring bias that might preferentially populate low j states. This effect is clearly much stronger in HF than in N_2 because of the larger energy separation of each j state of OH. Energy level separations are directly proportional to the magnitude of the rotational constants of the molecules of the ensemble and so the effect of an energy factor on T_r will be inversely proportional to the magnitude of B for a particular species. In Table II the ratio B_{CD}/B_{AB}, is listed where CD is the excited species and AB the bath molecule and is the *energy factor* which, along with other potential causes of variation in T_r, described below will be compared to the computed T_r data.

B. Efficiency factor

In an earlier articles[11] we introduced the concept that diatomic molecules may be classified according to their efficiency in converting orbital angular momentum of impact into molecular rotation and, simultaneously, kinetic energy of relative motion into rotational energy. For diatomic molecule AB and collision pair AB–CD, the energy conversion process is expressed by

$$\frac{1}{2}\mu_{AB-CD}v_r^2 = \frac{j^2}{2I} = \frac{j^2}{2\mu_{AB}r_{AB-CD}^2}. \quad (5)$$

Rearranging this equation,

$$j = \sqrt{\mu_{AB}\mu_{AB-CD}}r_{AB}v_r. \quad (6)$$

The optimal conversion of linear-to-angular momentum is when

$$j = \mu_{AB-CD}b_n^{max}v_r \quad (7)$$

Combining Eqs. (6) and (7) allows an efficiency factor F_{ABCD} for diatomic–diatomic rotational transfer from $j = 0$ to be defined as

$$F_{ABCD} = \frac{2b_n^{max}}{r_{AB}} = 2\sqrt{\frac{\mu_{AB}}{\mu_{AB-CD}}}. \quad (8)$$

Thus, the efficiency of conversion of kinetic energy and linear momentum to molecular rotation is proportional to the (square root of the) ratio of target molecule reduced mass to that of the collision pair. Thus, in Table II the *efficiency factor* is defined as $\sqrt{\mu_{AB}}/\sqrt{\mu_{AB\text{-}CD}}$. We have shown[26] in single collision studies that the probability of RT within a given molecule depends strongly on reduced mass of the collision pair. For example, increasing collision pair reduced mass is found to reduce rotational transfer cross sections. This arises because increased $\mu_{AB\text{-}CD}$ increases the effect of energy constraints on AM generation and hence reduces effective b_n^{max}. This prediction is found to agree with experimental observations.[27] A related reduction in RT probabilities is seen as initial j-state increases, again the result of energy constraints that arise as the cost of unit Δj increases. For the case $j_i > 0$, a more complex form of Eq. (8) is needed but at its core is the critical $\sqrt{}$reduced mass ratio.

Table II lists the binary gas ensembles that have been considered in this study, the mean value of T_r over the final 500 collision cycles of the computation for each species, and the ratio T_r^{AB}/T_r^{BC}. Reproducibility in individual calculated T_r values for each data point in the equilibrated region of ensemble evolution is of the order of $\pm 10\%$ for the minor species and $\pm 5\%$ for the bath molecules. The final two columns list efficiency factor and energy factor for each pair, calculated as described above. In terms of physical processes, the efficiency factor measures how effectively the orbital angular momentum of relative motion of the diatom–diatom pair couples to the rotational AM of each molecule. The energy factor differs in that it is simply a measure of the energy required to generate a single quantum of rotation within a given molecule. Thus, in terms of our theoretical model, the former is connected with the motive force for change, while the latter affects the energy constraints upon the primary mechanism.

It is worth recalling at this point that Boltzmann-like behaviour requires transitions between individual microstates be equally probable. The factors influencing collision-induced state-to-state population transfer discussed above, suggest this criterion will not be met for rotationally inelastic collisions. The origin of this in the case of the efficiency factor is readily seen from the velocity–angular momentum diagram of Fig. 4. In both collision systems represented, the dominant constraint is energetic for all values of Δj. The A-plot in these diagrams represents the threshold condition, i.e., b_n^{max} in Eq. (4). However, it is evident that for some lower maximum value of $b_n < b_n^{max}$, both energy and AM conditions may simultaneously be obeyed. Furthermore, this new maximum value of b_n is Δj channel dependent, as the diagrams of Fig. 4 make clear. In effect, this restricts the range of acceptable mutual geometries of the colliding diatom–diatom pair, a restriction that is made more difficult to overcome because energy and AM conservation conditions apply to the totality of change, i.e., changes in the internal states of each participating diatomic and of orbital AM of recoil. Thus, there is a conflict between the Boltzmann equiprobable microstate condition and the reality of energy and AM needs in each microscopic collision-induced state-to-state process.

From Table II it can be seen clearly that the efficiency factor is a reliable predictor of T_r ratio over the range of molecular pairs we have considered. The accuracy with which it matches the T_r ratio is quite striking. *This suggests strongly*

that the principal determinant of rotational temperatures in gas ensembles is the efficiency of coupling of orbital AM, generated on collision by molecules of the bath, with molecules of the ensemble, including other bath molecules. That program-related factors such as computational errors and rounding-up factors contribute cannot be ruled out but these would be present in all of our computations. The exceptionally low values of T_r seen here are limited to collision partners in the bath of N_2 molecules that have very low reduced mass and are absent for species with μ values close to that of N_2.

Thus, a physically sound justification is available for the very different final rotational temperatures seen in our computational model of gas ensembles when molecules of widely differing reduced mass are involved. Our findings suggest that the very low T_r values calculated here and in recent articles[3,4] for OH in an air-like mixture are likely to be reliable for the ensemble conditions we define.

IV. CONCLUSIONS

Figure 1 and similar data obtained on OH in a range of gases[3,4] make clear that under the conditions that apply to our ensembles, rotational temperatures at equilibrium rarely match those of translation or vibrational modes. When species such as HF or OH are present, the discrepancies can be very marked indeed with T_r particularly strongly affected. We have presented data from a series of studies designed to demonstrate that (i) this marked effect on T_r of molecules having low reduced mass is real under the ensemble conditions of our model and (ii) there is a consistent explanation for exceptionally low values of T_r based on competition for the orbital angular momentum and kinetic energy available, on collision, with bath gas molecules. For HF(6;4) in a bath of N_2(0;10) the ratio T_r^{N2}/T_r^{HF} is little changed over the range 100–2000 K. Further, the partitioning of rotational energy and AM between HF and N_2 changes little when initial excess energy is state specifically located in the minor component compared to when it is initially present as translational energy. These findings suggest that caution may be necessary when relating temperatures obtained from the rotational distributions in molecules of low reduced mass to those of other modes of species present. Though generally somewhat lower than translational temperatures, the vibrational temperature appears to be a better guide to an overall ensemble kinetic temperature than T_r for molecules having $\mu < 2$ amu.

[1] A. J. McCaffery and R. J. Marsh, J. Chem. Phys. **132**, 074304 (2010).
[2] A. J. McCaffery, M. Pritchard, J. F. C. Turner, and R. J. Marsh, J. Chem. Phys. **134**, 044317 (2011).
[3] A. J. McCaffery, M. Pritchard, J. F. C. Turner, and R. J. Marsh, J. Phys. Chem. A **115**, 4169 (2011).
[4] A. J. McCaffery, M. Pritchard, J. F. C. Turner, and R. J. Marsh, Chem. Phys. Lett. **515**, 302 (2011).
[5] See, for example, *Applied Combustion Diagnostics*, edited by K. Kohse Höinghaus and J. B. Jeffries (Taylor & Francis, New York, 2007); Jürgen Wolfrum, Faraday Discuss. Chem. Soc. **119**, 1 (2002).
[6] O. Lucas, Z. T. AlWahabi, V. Linton, and K. Meeuwissen, Appl. Spectrosc. **61**, 424 (2007).
[7] R. P. Wayne, *Chemistry of Atmospheres*, 3rd ed. (Oxford University Press, Oxford, 2000).
[8] A. B. Meinel, Astrophys. J. **112**, 555 (1950).
[9] P. C. Cosby and T. G. Slanger, Can. J. Phys. **85**, 77 (2007).
[10] R. J. Marsh and A. J. McCaffery, J. Chem. Phys. **117**, 503 (2002).
[11] A. J. McCaffery and R. J. Marsh, J. Phys. B **34**, R131 (2001); A. J. McCaffery, Phys. Chem. Chem. Phys. **6**, 1637 (2004).
[12] R. J. Marsh and A. J. McCaffery, J. Phys. B **36**, 1363 (2003).
[13] R. J. Marsh and A. J. McCaffery, Chem. Phys. Lett. **335**, 134 (2001).
[14] T. G. Kreutz and G. W. Flynn, J. Chem. Phys. **93**, 452 (1991).
[15] P. W. Atkins, *Physical Chemistry*, 5th ed. (Oxford University Press, Oxford, 1994), pp. 696–697.
[16] E. R. Serkin and G. C. Pimentel, J. Chem. Phys. **75**, 604 (1981).
[17] G. D. Downey, D. W. Robinson, and J. H. Smith, J. Chem. Phys. **66**, 1685 (1977).
[18] D. R. Smith, W. H. M. Blumberg, R. M. Nadille, S. J. Lipson, E. R. Huppi, and N. B. Wheeler, Geophys. Res. Lett. **19**, 593, doi:10.1029/92GL00396 (1992).
[19] A. J. McCaffery and R. J. Marsh, J. Chem. Phys. **132**, 074304 (2010).
[20] C. Flament, T. George, K. A. Meister, J. C. Tufts, J. W. Rich, V. V. Subramaniam, J. P. Martin, B. Piar, and M. Y. Perrin, Chem. Phys. **163**, 241 (1992).
[21] G. Hancock, R. Peverall, G. A. D. Ritchie, and L. J. Thornton, J. Phys. D: Appl. Phys. **39**, 1846 (2006).
[22] T. Seeger and A. Leipertz, Appl. Opt. **35**, 2665 (1996).
[23] C. Ottinger, A. F. Vilesov, and D. D. Xu, J. Chem. Phys. **102**, 1673 (1995); R. Bachmann, X. Li, C. Ottinger, and A. F. Vilesov, *ibid.* **96**, 5151 (1992); R. Bachmann, X. Li, C. Ottinger, A. F. Vilesov, and V. Wulfmeyer, *ibid.* **98**, 8606 (1993).
[24] N. A. Besley, A. J. McCaffery, M. A. Osborne, and Z. T. Rawi, J. Phys. B **31**, 4267 (1998).
[25] K. P. Huber and G. Herzberg, *Molecular Spectra and Molecular Structure IV Constants of Diatomic Molecules* (Van Nostrand, New York, 1979).
[26] S. Clare, A. J. Marks, and A. J. McCaffery, J. Chem. Phys. **111**, 9287 (2000).
[27] S. M. Clegg, A. B. Burrill, and C. S. Parmenter, J. Phys. Chem. A **102**, 8477 (1997).